

**Non-Hermitian scattering theory: Resonant tunneling probability amplitude in a quantum dot**

Hadas Barkay, Edvardas Narevicius, and Nimrod Moiseyev\*

*Department of Chemistry and Minerva Center of Nonlinear Physics in Complex Systems, Technion-Israel Institute of Technology, Haifa 32000, Israel*

(Received 30 July 2002; revised manuscript received 30 September 2002; published 30 January 2003)

We suggest a mechanism for the sharp phase change in the transition-probability amplitude of electrons scattered through a quantum dot. The proposed mechanism is a single electron phenomenon that involves interference between the two-dimensional resonances of the quantum dot. The dimensionality of the problem plays a key role in our mechanism.

DOI: 10.1103/PhysRevB.67.045322

PACS number(s): 72.10.-d, 73.40.-c, 73.21.La, 73.23.Hk

**I. INTRODUCTION**

Quantum dots play an important role in nanoscaled electronic devices. In order to fully understand the transport properties of quantum dots, phenomena such as tunneling of electrons must be characterized.

Phase measurements of an electron traversing a quantum dot via a double-slit interference experiment were carried out by Heiblum and co-workers.<sup>1,2</sup> In their experiment, the quantum dot (QD) was inserted into one slit, in a manner that enabled them to control the potential of the electrons trapped in it (by varying the plunger potential,  $V_p$ ). The second slit served as a reference. The measured transition probability,  $|t|^2$ , oscillated as a function of the plunger potential,  $V_p$ . When the scattered electron passed through a resonance state, the transition probability exhibited a Lorentzian-shaped peak, and the phase of the transition-probability amplitude changed by  $\pi$ , as expected by the Breit-Wigner model for resonant tunneling. Surprisingly, the phase does not accumulate but oscillates: although in each resonance the phase changes by  $\pi$ , between resonances it drops sharply by  $\pi$ . In spite of intense work on this problem<sup>3-11</sup> to the best of our knowledge there is no satisfactory explanation of this phenomenon. Most of the calculations which have been carried out are either for particle space model Hamiltonians or for general mathematical models based on the Friedel sum rule combined with time-reversal symmetry. The conclusion from these studies is that in true one-dimensional (1D) systems the sharp phase drops by  $\pi$  in the tail of the resonant peak that never occurs. Such a phenomenon is obtained, however, for single electron transport for quasi-1D systems. This result was obtained also in simulation calculations for a real-space model Hamiltonian with a 2D box potential (single-crossbar cavity).<sup>5</sup> The discontinuity in the phase evolution of electron transport in the single-crossbar cavity is associated with the interference between two different transmission channels belonging to a localized state in the 2D potential and a continuous state of the transmission channel. An open question we would like to address is whether the discontinuity in the phase evolution would happen also for analytical 2D potential surfaces. Another question we would like to answer is whether the discontinuity in the phase evolution can happen due to another mechanism. As we will show here for analytical 2D potentials a sharp drop (not a discontinuity) by  $\pi$  happens due to the interference between adjacent resonance

states associated with the double barrier potential in the adiabatic 1D potential which does not exist in the 2D single-crossbar cavity QD model Hamiltonian.

The phenomenon in which the phase drops sharply by  $\pi$  at transmission zeros has been associated with the fact that in quasi-1D systems the even and odd resonance levels do not necessarily alternate in energy.<sup>7,9</sup> It is a common belief that whenever the transmission coefficient reaches zero, the phase has a sharp drop by  $\pi$ . As we will show here this is indeed a necessary condition but not a sufficient one.

In our work we study single electron transport for a real-space 2D model Hamiltonian. The potential we introduce is a 2D one-electron effective QD model Hamiltonian that simulates the QD in Heiblum's experiment. Unlike the single-crossbar cavity used before, our 2D potential is an analytical function. In our model the transition of the electron from the entrance channel to the exit one through the QD is hindered by two potential barriers that do not appear in the single-crossbar cavity model.

We obtained that for the adiabatic 1D double barrier potential, the transition probability amplitude behaves in a similar way when varying the scattered electron energy,  $E$ , or the depth of the well between the two barriers (via the variation of  $V_p$ ). Since the numerical calculations are simpler for the variation of the scattered electron energy rather than the variation of  $V_p$ , we address ourselves here to the following question: how does the transition-probability amplitude change as a function of the energy of the scattered electron,  $E$ , when  $V_p$  is held fixed?

In order to answer this question we have used the complex adiabatic approach.<sup>12</sup> First the complex resonance potential-energy surfaces were calculated as a function of the slow coordinate (which is perpendicular to the propagation coordinate). Then, assuming that the electron scattering proceeds via a single potential-energy surface (PES), the transition-probability amplitude,  $t(E)$ , was calculated.

**II. 2D ONE-ELECTRON EFFECTIVE QD MODEL HAMILTONIAN**

We propose an effective one-electron two-dimensional model potential of the QD, which preserves the main characteristics of the QD in the Heiblum experiment. That is, (i) the entrance channel, entrance barrier, potential well, exit barrier, and exit channel are clearly defined (see Fig. 1); (ii)

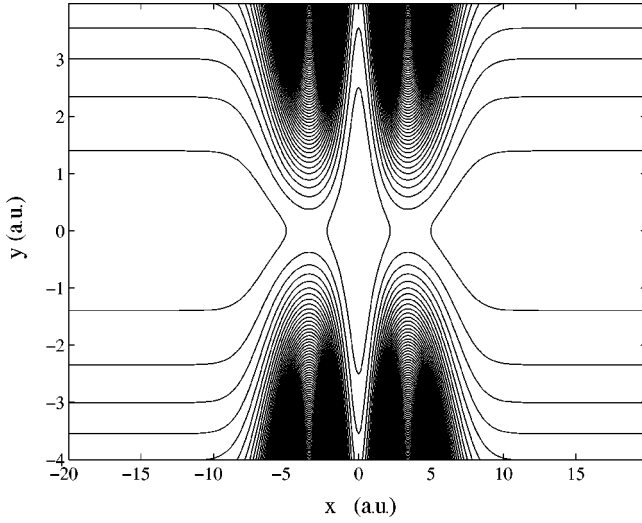


FIG. 1. The two-dimensional QD potential-energy surface,  $V(x,y)$ , defined in Eq. (2). Note the entrance and exit channels, entrance and exit barriers, and the QD embedded between the barriers. Parameters:  $\mu_e=1$ ;  $V_0=0.5$ ;  $\alpha=1.6$ ;  $\gamma=0.1$ ;  $V_p=0$ ;  $\lambda=0.75$ ;  $w_\infty=1$ ;  $a=0.76215$ ;  $b=0.32802$ ;  $c=0.08871$ . The parameters  $a, b$ , and  $c$  were calculated according to the geometry of the QD in Heiblum's experiment.  $\lambda$  was chosen to allow the control on the depth of the QD well by a single parameter,  $V_p$ , without changing the height of the barriers.

there are similar geometrical proportions; (iii) the potential surface supports at least one bound state inside the potential well, and supports isolated resonance states (i.e.,  $\Gamma_j < |E_j - E_{j\pm 1}|$ ); and (iv) the depth of the potential well is controlled by a single parameter, the plunger potential parameter  $V_p$ , which has a minor effect on the geometry of the QD. By increasing  $V_p$ , the number of bound states in the open QD is increased.

The two-dimensional QD model Hamiltonian, where  $x$  is the propagation coordinate, is given by

$$\hat{H}(x,y) = \frac{\hat{p}_x^2}{2\mu_e} + \frac{\hat{p}_y^2}{2\mu_e} + V(x,y), \quad (1)$$

where  $\mu_e$  is the effective electron mass and the PES is given by

$$V(x,y) = V(x) + \frac{\mu_e}{2} y^2 \omega^2(x), \quad (2)$$

where

$$V(x) = V_0(x^2 - \alpha)e^{-\gamma x^2} - V_p e^{-\lambda x^2},$$

$$\omega(x) = \omega_\infty + a(x^2 - b)e^{-cx^2}.$$

$\omega_\infty$  is the frequency of the harmonic motion of the free electron in the confined direction ( $y$  coordinate) in the entrance/exit channels.

The potential parameters used in our calculations are given in the caption of Fig. 1. A one-dimensional cut through the PES defined above at a constant  $y$  gives a potential,  $V(x;y)$ , which has a well between two separated potential

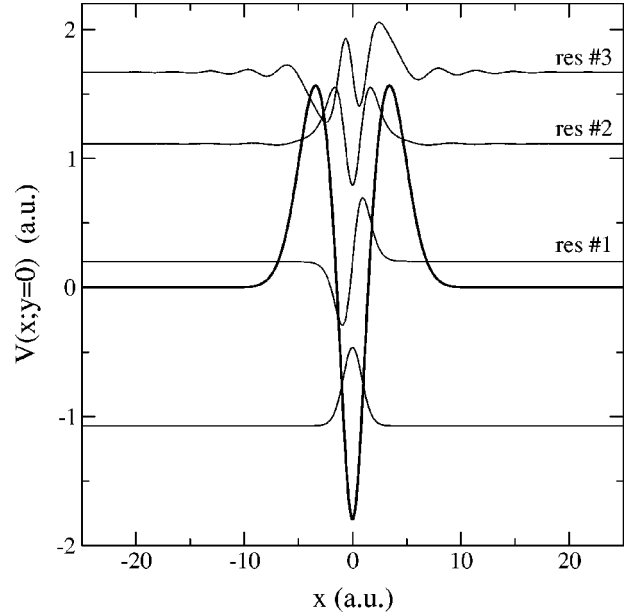


FIG. 2. The 1D potential in the  $x$  direction,  $V(x;y=0)$ , when  $V_p=1$ . The bound and isolated narrow resonance complex-scaled wave functions (real part) are plotted for  $\theta=0.13$ .

barriers. These 1D potentials support at least one bound state and a few isolated resonance states (see Fig. 2).

### III. TRANSITION-PROBABILITY AMPLITUDES IN THE 2D QD MODEL HAMILTONIAN

The transition-probability amplitude,  $t(V_p)$ , in the 1D case, has been calculated using non-Hermitian scattering theory.<sup>13</sup> It shows a series of resonance peaks [see Fig. 3(a)]. The phase of  $t(V_p)$  changes by  $\pi$  in resonances and accumulates between resonances [see Fig. 3(b)]. The sharp phase drop is not observed. Our calculations show that this phase drop cannot be explained by 1D one-electron calculations, even when interference between different paths (different  $y$  cuts) is taken into consideration. Therefore, it is clear that two dimensions are needed to obtain the sharp phase drop phenomenon when using an effective one-electron model.

As was mentioned above, the 1D transition-probability amplitude,  $t(E)$ , which is obtained when  $V_p$  is held fixed and the energy of the incoming electron,  $E$ , is varied, behaves similarly to the 1D transition-probability amplitude  $t(V_p)$ . Regardless of the dimensionality of the studied problem, the computational effort needed to calculate  $t(V_p)$  is much larger than the one needed to calculate  $t(E)$ . This is because the major numerical effort lies in the construction of the spectral representation of the Green operator, which requires the diagonalization of the Hamiltonian for every  $V_p$ . Therefore, we will concentrate on  $t(E)$  in the 2D case.

We have used non-Hermitian scattering theory to calculate the transition-probability amplitude, within the framework of the complex adiabatic approach. It should be stressed that non-Hermitian quantum mechanics allows us to use complex adiabatic potential-energy surfaces in cases where one has to go beyond the adiabatic approximation in

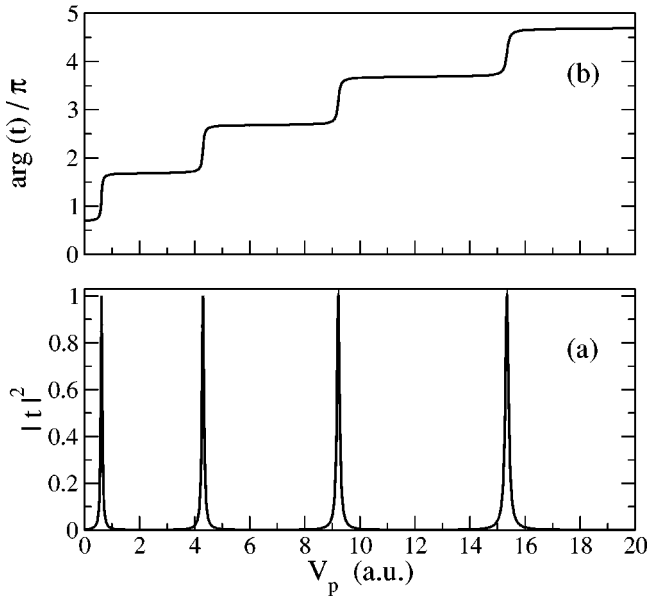


FIG. 3. Transition probability for the 1D cut  $V(x;y=0)$  as a function of  $V_p$ , when the scattering energy is held fixed,  $E=1.2$  a.u. (this energy is below the barrier height for any value of  $V_p$ ). (a) The transition probability,  $|t|^2$ , exhibits a series of peaks which corresponds to the resonances. (b) The phase of the transition-probability amplitude,  $\arg(t)$ , jumps by  $\pi$  in each resonance and accumulates as  $V_p$  is varied.

Hermitian quantum mechanics (QM).<sup>14,15</sup> In the adiabatic approximation, we assume that the motion in the  $y$  direction is much slower than in the  $x$  direction. This assumption is based on the geometry of the two-dimensional potential surface (see Fig. 1).

Using the adiabatic approximation, the Hamiltonian in the  $x$  direction, for a given  $y$ , is given by

$$\hat{H}(x;y) = -\frac{\hbar^2}{2\mu_e} \frac{\partial^2}{\partial x^2} + V(x;y). \quad (3)$$

We use complex scaling, i.e.,  $x \rightarrow xe^{i\theta}$ , to calculate the solutions of the complex-scaled Schrödinger equation. The use of complex scaling (i.e., non-Hermitian QM) enables us to associate a resonance state with a single eigenstate of the Hamiltonian, while in Hermitian QM a resonance state is associated with a wave packet (which is not an eigenstate of the Hermitian Hamiltonian). Therefore by complex scaling we get

$$\hat{H}(xe^{i\theta};y)\psi_\theta^j(x;y) = E^j(y)\psi_\theta^j(x;y). \quad (4)$$

The complex eigenenergies,  $E^j(y)$ , which correspond to the resonance states are  $\theta$  independent, provided  $\theta$  is sufficiently large. The resonance states,  $\psi_\theta^j(x;y)$ , are square integrable (see Fig. 2) and  $\theta$  dependent.

Within the framework of the non-Hermitian adiabatic approximation, separate complex resonance potential-energy surfaces are defined by

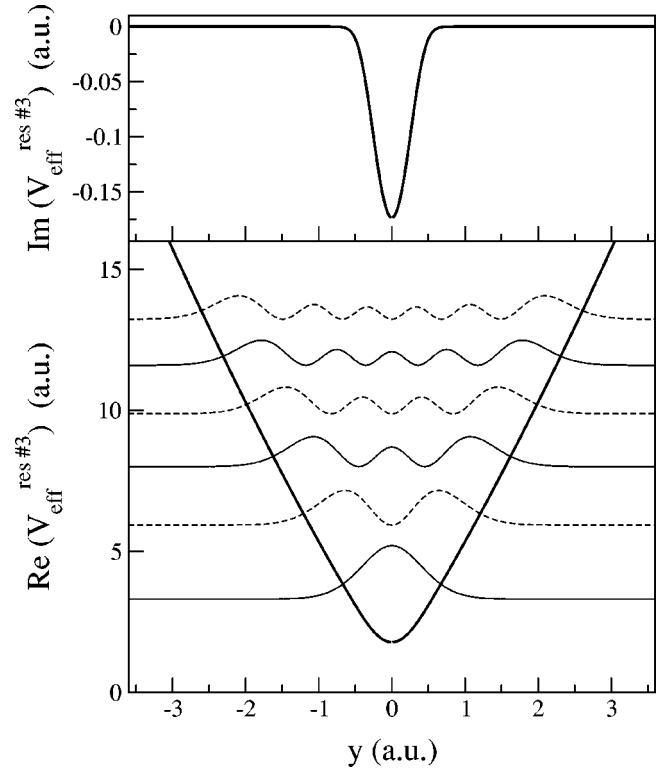


FIG. 4. The 1D effective complex resonance PES in the  $y$  direction, for resonance 3, when  $V_p=0$ . The first seven eigenstates,  $|\chi_n^j(y)|^2$ , are plotted with normal/dashed lines, according to the symmetry of the eigenstate.

$$V_{\text{eff}}^j(y) \equiv E^j(y) \equiv \epsilon^j(y) - \frac{i}{2} \Gamma^j(y). \quad (5)$$

For the  $j$ th resonance surface, the effective Hamiltonian in the  $y$  direction is given by

$$\hat{H}_{\text{eff}}^j(y) = -\frac{\hbar^2}{2\mu_e} \frac{\partial^2}{\partial y^2} + V_{\text{eff}}^j(y). \quad (6)$$

By solving the eigenvalue problem,

$$\hat{H}_{\text{eff}}^j(y)\chi_n^j(y) = e_n^j\chi_n^j(y), \quad e_n^j \equiv \epsilon_n^j - \frac{i}{2}\gamma_n^j, \quad (7)$$

the complex resonance eigenstates and eigenenergies were calculated. The complex eigenenergies,  $e_n^j$ , provide the energy positions,  $\epsilon_n^j$ , and widths,  $\gamma_n^j$  (which correspond to the inverse of the lifetimes of the resonance states) of the temporarily trapped electron in the QD.

In Fig. 4 we show an effective complex resonance PES and the corresponding resonance eigenstates. The transition-probability amplitude is calculated using the Lippmann-Schwinger equation

$$t_{i \rightarrow f}(E) = (\Psi_i | V + VG V | \Psi_f), \quad (8)$$

where  $\Psi_i$  and  $\Psi_f$  are the initial and final wave functions of the scattered electron. Under the adiabatic approximation  $\Psi_{i,f}$  can be presented as

$$\Psi_{i,f}(x,y) = \Theta_{i,f}(x;y) \varphi_{i,f}(y), \quad (9)$$

where  $\Theta$  is the wave function of the scattered electron in the  $x$  direction:

$$\Theta_{i,f}(x;y) = \sqrt{\frac{\mu_e}{\hbar^2 k_{i,f}}} e^{ik_{i,f}x},$$

$$k_{i,f} = \sqrt{2\mu_e[E - e_{i,f}^\infty - E_{th}(y)]}, \quad (10)$$

and  $\varphi_{i,f}$  are the asymptotic wave functions of the scattered electron in the  $y$  direction (in our case, this is eigenstates of a harmonic oscillator with the frequency  $w_\infty$ ).

Assuming tunneling is assisted by the  $j$ th effective resonance potential surface, for the case where the quantum state of the scattered electron remains unchanged (i.e.,  $i=f$ ), the transition-probability amplitude is given by

$$t_{i \rightarrow i}^j = \sum_n \frac{[\varphi_i(y) | \sqrt{\Gamma^j(y)} | \chi_n^j(y)] [\chi_n^j(y) | \sqrt{\Gamma^j(y)} | \varphi_i(y)]}{E - e_i^\infty - e_n^j}. \quad (11)$$

For derivation of this equation see Ref. 12. The notation  $(\dots | \dots)$  stands for the generalized inner product which is used in non-Hermitian QM, where  $(f|g) \equiv \langle f^* | g \rangle$ . Note that the eigenenergies,  $e_n^j$ , and eigenstates,  $\chi_n^j(y)$ , are complex due to the complex effective resonance potential. This formula can be generalized for any initial and final states by replacing  $\sqrt{\Gamma^j(y)}$ , which was defined in Eq. (5), by the partial width amplitude of the  $j$ th resonance state. This approach should also be used if one wants to take into account tunneling assisted by more than one resonance complex PES.

The calculated transition-probability amplitude,  $t_{0 \rightarrow 0}^j$ , is shown in Fig. 5. The transition probability shows a series of Lorentzian resonance peaks. Those appear when the energy of the incoming electron in the  $x$  direction,  $E - e_i^\infty$ , is close to the real part of the resonance energy,  $e_n^j$ . Due to the symmetry of the problem, tunneling is allowed only through even resonance states.

Two distinct phenomena can be observed in Fig. 5(b), which shows the absolute value of the transition-probability amplitude, as a function of the incoming electron energy,  $E$ . First, the width of the resonance peaks decreases as  $E$  increases. Second, the height of the resonance peaks decreases as  $E$  increases.

The explanation for both phenomena is based on the Breit-Wigner model for resonant tunneling. In the vicinity of a narrow isolated resonance (i.e.,  $\gamma_n < |\epsilon_n - \epsilon_{n\pm 1}|$ ), the transition-probability amplitude is given by the leading term of  $t(E)$  in Eq. (11):

$$T^j(E) \equiv |t^j(E)|^2 = \left| \frac{[\varphi_i(y) | \sqrt{\Gamma^j(y)} | \chi_n^j(y)]}{E - e_i^\infty - e_n^j} \right|^2 \equiv \left| \frac{C_n^j}{\gamma_n^j} \right|^2. \quad (12)$$

Regarding the width of the resonance peaks, the width is associated with the inverse of the lifetime of the resonance states. The maximum of the amplitude of  $\chi_n^j$  is at  $y=0$  for the first resonance state ( $n=0$ ) and moves toward the clas-

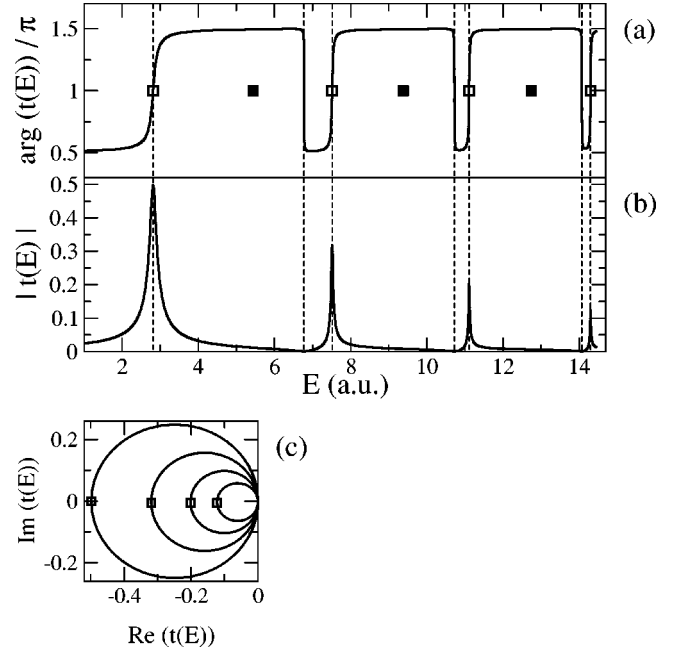


FIG. 5. Transition-probability amplitude,  $t_{0 \rightarrow 0}(E)$ , assisted by the third effective complex resonance potential-energy surface. (a) Phase, (b) absolute value, and (c) trajectory. The phase changes by  $\pi$  in resonances. The phase drops by  $\pi$  between resonances, when  $t(E)$  intersects the origin. The position of resonance states is plotted with squares (open squares—symmetric resonance states, full squares—antisymmetric resonance states). Note that due to the symmetry properties of the problem, transition is not assisted by antisymmetric resonances.

sical turning points of  $\text{Re}[V_{\text{eff}}^j(y)]$  as  $n$  is increased (see Fig. 4). Due to the shape of the PES (see Fig. 1), the temporarily trapped electron in the QD tunnels out along the  $x$  direction mostly around  $y=0$ . For higher values of  $|y|$  the tunneling is hindered by the potential barriers. Therefore, the lifetime of the resonance states increases as  $n$  increases, and the corresponding widths decrease. Note that the width of the resonance peak in the transition-probability graph can be associated with the inverse of the lifetime of the resonance state only if the resonances are isolated, otherwise interference phenomena between overlapping resonance states may change the Lorentzian shape of the resonance peaks.

Concerning the height of the resonance peaks, Eq. (12) shows that the height is proportional to the probability of populating the  $n$ th resonance state. This probability is given by the overlap  $C_n^j \equiv |[\varphi_0(y) | \sqrt{\Gamma^j(y)} | \chi_n^j(y)]|^2$ , where  $\varphi_0(y)$  is the initial state and  $\Gamma^j(y)$  is given by the imaginary part of the resonance surface [see Eq. (11)]. As described above, the maximal amplitude of  $\chi_n^j$  changes from  $y=0$  for the first resonance state to the classical turning points of  $\text{Re}(V_{\text{eff}}^j(y))$  as  $n$  is increased.  $\Gamma^j(y)$  is localized around  $y=0$ , and  $\varphi_0(y)$ , which is the ground state of a harmonic oscillator with the frequency  $w_\infty$ , gets a maximum around  $y=0$ . Therefore,  $C_n^j$  decreases as  $n$  is increased. The height of the resonance peaks is also inversely proportional to the width of the resonance state,  $\gamma_n^j$ , which decreases as  $n$  increases. Despite this dependence, the transition probability in resonance is domi-

nated by the overlap and decreases as  $n$  is increased. Note that we discuss here only the resonance contribution to the transition-probability amplitude and ignore the direct-scattering process which dominates the high-energy regime.

The phase of the transition-probability amplitude,  $\arg[t(E)]$ , changes by  $\pi$  when  $|t(E)|$  exhibits a maximum [see Fig. 5(a)]. This well-known phenomenon can be explained by the Breit-Wigner model for resonant tunneling.

The phase drops abruptly by  $\pi$  between resonance peaks, when the complex transition-probability amplitude,  $t(E)$ , intersects the origin, i.e.,  $t(E) = 0 + i0$ . This result is similar to the association of the sharp phase drop by  $\pi$  in the tail of the resonant peak.<sup>7,16</sup> Note, however, that we obtained the sharp phase drop as a result of interference between two neighboring 2D resonance states which decay through the two potential barriers located at the entrance and the exit channels. This interference which leads to the sharp phase drop in  $t(E)$  cannot occur in 1D double barrier potentials as we will explain below.

The energy where zero transmission is obtained is given approximately by the position of the intersection of two neighboring Lorentzian peaks ( $n, n+1$ ). The position of the intersection is determined by the population of the corresponding resonance states and by their widths. On the basis of the analysis given above, the intersection is at an energy closer to the  $n+1$  resonance peak (which is narrower and less populated than the  $n$ th one). The energy  $E_0$  at which  $t(E_0) = 0 + i0$  can be approximately obtained by taking into account the interference between two adjacent resonance states,

$$\frac{C_n^j}{E_0 - e_i^\infty - e_n^j} + \frac{C_{n+1}^j}{E_0 - e_i^\infty - e_{n+1}^j} = 0. \quad (13)$$

Our calculations show that this approximation holds in the case presented in Fig. 5, though there is a slight deviation due to interference effects with other resonance states.

Why does the phase of  $t(E)$  change abruptly by  $\pi$  when  $t(E)$  intersects the origin? Expanding the transition-probability amplitude in a Taylor series around an intersection energy,  $E_0$ , gives

$$t(E_0 \pm \varepsilon) = t(E_0) + \left. \frac{dt(E)}{dE} \right|_{E_0} (\pm \varepsilon) + \frac{1}{2} \left. \frac{d^2t(E)}{dE^2} \right|_{E_0} (\pm \varepsilon)^2 + \dots \quad (14)$$

When  $t(E_0) = 0$  and when  $\varepsilon$  is small enough, if  $dt(E)/dE|_{E_0} \neq 0$  as in our case, we get

$$t(E_0 \pm \varepsilon) = \pm \varepsilon \left. \frac{dt(E)}{dE} \right|_{E_0}. \quad (15)$$

This equality implies that in a very short energy range the phase changes by  $\pi$ . This is proof that it is not necessarily true that whenever the transmission coefficient reaches zero, the phase has a sharp drop by  $\pi$ . The zero transmission coefficient,  $t(E_0) = 0$ , is a necessary condition for the sharp

phase drop by  $\pi$  at the tail of the resonant peak but it is not a sufficient one. This abrupt phase change happens at zero transmissions if and only if  $dt(E)/dE|_{E_0} \neq 0$ .

Figure 5(c) shows the trajectory of  $t(E)$ . At each one of the intersection energies the imaginary axis is tangent to  $t(E)$  at the origin. Therefore, the first derivative of  $t(E)$  is almost a pure imaginary number, and  $t(E_0 \pm \varepsilon) = +i\delta$ . Since in our numerical calculations  $t(E)$  does not intersect the origin but passes very close to it as  $E$  is varied, the phase changes smoothly from  $-\pi/2$  to  $\pi/2$  instead of jumping.

The Taylor expansion of  $t(E)$  shows that the transition probability does *not* jump by  $\pi$  when  $t(E)$  intersects the origin whenever two conditions are satisfied simultaneously: (i)  $t(E_0) = 0$ ; (ii)  $dt(E)/dE|_{E_0} = 0$ . In the 2D case discussed above, when  $t(E)$  can be approximately obtained by taking into account only two adjacent resonance states [see Eq. (13)], it is impossible to satisfy simultaneously both conditions. Therefore, whenever this approximation is valid the intersection of  $t(E)$  with the origin implies a sudden change of the phase of  $t(E)$  by  $\pi$ . Our calculations for a 1D model Hamiltonian<sup>13</sup> have shown that in 1D problems one cannot neglect the interference of the resonances with the scattering background. Therefore, in a 1D problem it is possible to satisfy both conditions and the phase of  $t(E)$  does not jump by  $\pi$  when  $t(E)$  intersects the origin. This is another explanation for the fact that the phase drop by  $\pi$  at the tail of the resonant peak *cannot* be obtained in single electron transport through a double barrier 1D potential.

#### IV. CONCLUSIONS

The electron-scattering transition-probability amplitude through an open QD,  $t(E)$ , has been studied for a real-space 2D model Hamiltonian. A sharp change of the phase of  $t(E)$  by  $\pi$  occurs when  $t(E)$  intersects the origin. It implies that two conditions should be satisfied in order to observe a sharp drop of the phase by  $\pi$  in the tail of the resonant peak. One condition is  $t(E_0) = 0$ , whereas the second condition is  $dt(E)/dE|_{E_0} \neq 0$ . We have shown that this phase drop is a resonance interference phenomenon that happens even within the framework of a one-electron effective QD potential. The fact that the QD has at least two dimensions is a crucial point in the mechanism we have presented here. Our explanation of a sharp phase change is based on the destructive interference between neighboring resonances and thus differs from the mechanism based on the Fano resonance (see, for example, Refs. 5 and 11).

In this work we solved the Schrödinger equation and calculated the resonance wave functions for the 2D potential using the complex-scaling method. The advantage of this method is that it enables one to calculate the complex poles of the scattering matrix using computational methods that have been originally developed for bound-state problems. Complex scaling enabled the calculations of resonance states not only for 3D problems but also for many-body problems such as resonances of electronically excited  $H_2$  and the short-lived resonance of the negative hydrogen molecular ion. The use of the complex-scaling adiabatic approach (a first for the QD problem, to the best of our knowledge) sim-

plifies the numerical calculations. Using the complex-scaling adiabatic approach we believe that the resonances of the 3D *many*-electron QD problem can be calculated even when the electron correlation effect is taken into consideration.

Another point that should be emphasized is that in our calculations we have concentrated on the contributions of a resonance PES to the transition-probability amplitudes and ignored the direct-scattering process. As shown before, in a 1D problem the direct scattering can be neglected only at the resonance energies.<sup>13</sup> However, this is not the case in the 2D scattering experiment, where the relevant interfering resonances are associated with the confined motion perpendicular to the scattering direction. This is the key point of the phase-drop mechanism described in this work. Although the mechanism we have presented is relevant to the Heiblum

group experiments, it is not within the scope of the present paper to provide a full numerical simulation. Such simulations are under current study. We summarize by saying that we have suggested a one-electron effective two-dimensional model which exhibits the phase-drop phenomenon in the transition-probability amplitude and we provide the conditions which should be fulfilled in order to make it happen.

#### ACKNOWLEDGMENTS

This work was supported in part by the US-Israel Binational Science Foundation, by the Basic Research Foundation administered by the Israeli Academy of Sciences and Humanities, and by the Fund for the Promotion of Research at the Technion.

---

\*Electronic address: nimrod@tx.technion.ac.il

<sup>1</sup>A. Yacoby, M. Heiblum, D. Mahalu, and H. Shtrikman, Phys. Rev. Lett. **74**, 4047 (1995).

<sup>2</sup>R. Schuster, E. Buks, M. Heiblum, D. Mahalu, V. Umansky, and H. Shtrikman, Nature (London) **385**, 417 (1997).

<sup>3</sup>H. Q. Xu and W. D. Sheng, Phys. Rev. B **57**, 11 903 (1998).

<sup>4</sup>C. M. Ryu and S. Y. Cho, Phys. Rev. B **58**, 3572 (1998).

<sup>5</sup>H. W. Lee, Phys. Rev. Lett. **82**, 2358 (1999).

<sup>6</sup>T. Taniguchi and M. Büttiker, Phys. Rev. B **60**, 13 814 (1999).

<sup>7</sup>P. G. Silverstov and Y. Imry, Phys. Rev. Lett. **85**, 2565 (2000).

<sup>8</sup>A. L. Yeyati and M. Büttiker, Phys. Rev. B **62**, 7307 (2000).

<sup>9</sup>H.-W. Lee and C. S. Kim, Phys. Rev. B **63**, 075306 (2001).

<sup>10</sup>C.-M. Ryu and S. Y. Cho, Phys. Rev. B **58**, 3572 (1998).

<sup>11</sup>H. Q. Xu and B.-Y. Gu, J. Phys. C: Condens. Matter **13**, 3599 (2001).

<sup>12</sup>E. Narevicius and N. Moiseyev, J. Chem. Phys. **113**, 6088 (2000).

<sup>13</sup>H. Barkay and N. Moiseyev, Phys. Rev. A **64**, 044702 (2001).

<sup>14</sup>E. Narevicius and N. Moiseyev, Phys. Rev. Lett. **81**, 2221 (1998).

<sup>15</sup>E. Narevicius and N. Moiseyev, Phys. Rev. Lett. **84**, 1681 (2000).

<sup>16</sup>T. Chen, W. S. Liu, and S. J. Xiong, Commun. Theor. Phys. **35**, 121 (2001).